Unique Thickness-Dependent Properties of the van der Waals Interlayer Antiferromagnet $MnBi_2Te_4$ Films

M. M. Otrokov,[1,2,3,4,*] I. P. Rusinov,[5,4] M. Blanco-Rey,[6,3] M. Hoffmann,[7] A. Yu. Vyazovskaya,[5,4] S. V. Eremeev,[8,5,4] A. Ernst,[7,9] P. M. Echenique,[3,6,1] A. Arnau,[1,6,3] and E. V. Chulkov[1,6,3,4,†]

[1]*Centro de Física de Materiales (CFM-MPC), Centro Mixto CSIC-UPV/EHU, 20018 Donostia-San Sebastián, Basque Country, Spain*

[2]*IKERBASQUE, Basque Foundation for Science, 48011 Bilbao, Spain*

[3]*Donostia International Physics Center (DIPC), 20018 Donostia-San Sebastián, Basque Country, Spain*

[4]*Saint Petersburg State University, 198504 Saint Petersburg, Russia*

[5]*Tomsk State University, 634050 Tomsk, Russia*

[6]*Departamento de Física de Materiales UPV/EHU, 20080 Donostia-San Sebastián, Basque Country, Spain*

[7]*Institut für Theoretische Physik, Johannes Kepler Universität, A 4040 Linz, Austria*

[8]*Institute of Strength Physics and Materials Science, Russian Academy of Sciences, 634021 Tomsk, Russia*

[9]*Max-Planck-Institut für Mikrostrukturphysik, Weinberg 2, D-06120 Halle, Germany*

(Received 11 October 2018; published 13 March 2019)

Using density functional theory and Monte Carlo calculations, we study the thickness dependence of the magnetic and electronic properties of a van der Waals interlayer antiferromagnet in the two-dimensional limit. Considering $MnBi_2Te_4$ as a model material, we find it to demonstrate a remarkable set of thickness-dependent magnetic and topological transitions. While a single septuple layer block of $MnBi_2Te_4$ is a topologically trivial ferromagnet, the thicker films made of an odd (even) number of blocks are uncompensated (compensated) interlayer antiferromagnets, which show wide band gap quantum anomalous Hall (zero plateau quantum anomalous Hall) states. Thus, $MnBi_2Te_4$ is the first stoichiometric material predicted to realize the zero plateau quantum anomalous Hall state intrinsically. This state has been theoretically shown to host the exotic axion insulator phase.

DOI: 10.1103/PhysRevLett.122.107202

After the isolation of graphene, the field of two-dimensional (2D) van der Waals (vdW) materials has experienced an explosive growth and new families of 2D systems and block-layered bulk materials, such as tetradymite-like topological insulators (TIs) [1,2], transition metal dichalcogenides [3], and others [4–6] have been discovered. The remarkable electronic properties, along with the possibility of their tuning via thickness control, doping, intercalation, proximity effects, etc., make the layered vdW materials attractive from both practical and fundamental points of view. The relative simplicity of fabrication with a number of techniques has greatly facilitated a comprehensive study of these systems. However, the important step towards magnetic functionalization of the inherently nonmagnetic layered vdW materials and a controllable fabrication of the resulting hybrid systems has proven challenging. Therefore, aiming at exploring magnetism of layered vdW materials in the 2D limit, new possibilities have been considered. One of them is the ultrathin laminae exfoliation from intrinsically ferromagnetic (FM) vdW crystals, such as $Cr_2Ge_2Te_6$ and CrI_3, whose magnetic behaviour has been studied down to a few layers thickness [7,8]. An alternative fabrication strategy is epitaxial growth. With this technique, a 2D FM septuple layer (SL) block of $MnBi_2Se_4$ has been grown on top of the Bi_2Se_3 TI surface [9]. Similar systems have been theoretically proposed as a promising platform for achieving the quantized anomalous Hall (QAH) and magnetoelectric effects at elevated temperatures [10–12]. Later, epitaxial growth of the $Bi_2Se_3/MnBi_2Se_4$ multilayer heterostructure has been reported [13].

The field of 2D vdW magnets is in its infancy and many more materials with new properties are to be explored. In particular, vdW *antiferromagnets* are expected to be of great interest. Indeed, recently it has been reported that the layered vdW compound $MnBi_2Te_4$ is the first ever antiferromagnetic (AFM) TI [14]. This state of matter is predicted to give rise to exotic phenomena such as quantized magnetoelectric effect [15], axion electrodynamics [16], and Majorana hinge modes [17]. Moreover, the combination of magnetism with spin-orbit coupling, along with strong thickness dependence of electronic structure in the 2D limit suggest that vdW compounds like $MnBi_2Te(Se)_4$ and $MnSb_2Te_4$ [18] might be attractive for both fundamental and applied research. Finally, a novel type of energetically stable and universal interface between (A)FM and topological insulators has been proposed recently [19]. At such an interface, the film of magnetic material, that does not show vdW bonding intrinsically, turns out to be vdW-coupled to a TI as a result of immersion below the surface of the TI. Incidentally, the axion

 © 2019 American Physical Society

TH-2019-07

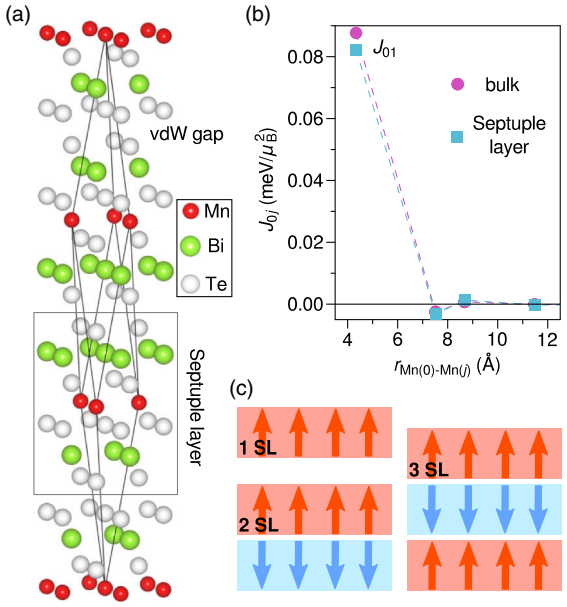

FIG. 1. (a) Atomic structure of the $R\bar{3}m$-group bulk $MnBi_2Te_4$ with red, green, and white balls showing Mn, Bi, and Te atoms, respectively. The paramagnetic rhombohedral unit cell is shown by black lines. (b) Calculated exchange constants J_{0j} for the intralayer pair interactions as a function of the distance $r_{Mn(0)-Mn(j)}$ for the bulk (circles) and free-standing SL (squares). (c) 1-, 2-, and 3-SL-thick $MnBi_2Te_4$ films, showing an FM, compensated AFM, and uncompensated AFM orders, respectively.

insulator state could also be achieved in such heterostructures [20]. These and other AFM systems appear to be interesting candidates to couple the emerging fields of AFM spintronics [21] and layered vdW materials [7,8].

In this Letter, using state-of-the-art *ab initio* techniques and the Monte Carlo method, we study the magnetic, electronic and topological properties of the layered vdW AFM TI compound $MnBi_2Te_4$ in the 2D limit. We find a unique set of thickness-dependent magnetic and topological transitions, which drive the $MnBi_2Te_4$ thin films through FM and (un)compensated AFM phases (see Fig. 1), with AFM states that give rise to QAH or zero plateau QAH effects.

The electronic structure calculations were carried out within density functional theory using the projector augmented-wave method [22] (VASP code [23,24]). The exchange-correlation energy was treated using the generalized gradient approximation [25]. The Hamiltonian contained scalar relativistic corrections and the spin-orbit coupling was taken into account [26]. To describe the vdW interactions, we used the DFT-D3 approach [27,28]. The Mn $3d$-states were treated employing the GGA + U approach [29,30]. The Heisenberg exchange coupling constants J_{ij} were computed *ab initio* using the full-potential linearized augmented plane waves method [31] (FLEUR code [32]). The magnetic critical temperatures were determined using Monte Carlo simulations based on a classical Heisenberg Hamiltonian parametrized with the magnetic anisotropy energies (MAEs) and J_{ij} constants obtained from *ab initio* calculations. The Chern numbers were determined using Z2PACK [33,34] and *ab-initio*-based tight-binding calculations [35,36]. The edge electronic band structure was calculated within the semi-infinite medium Green function approach. More details on methods can be found in the Supplemental Material I [37].

$MnBi_2Te_4$ is built of SL blocks stacked one on top of another along the [0001] direction and held together by vdW forces [14,48] [Fig. 1(a)]. As far as its magnetic order is concerned, it appears to be an interlayer antiferromagnet, where the FM Mn layers of neighboring blocks are coupled antiparallel to each other [14,18]. The reason for this AFM coupling between Mn layers is Anderson superexchange [49], which appears in nonmetallic solids due to the tendency of electrons to delocalize by spreading along non-orthogonal overlapping orbitals (see Supplemental Material II [37]).

Although the recently synthesized single crystals of $MnBi_2Te_4$ show some degree of statistical Mn/Bi disorder, our *ab initio* calculations indicate that such an intermixing is less favorable than the ideal structure (Supplemental Material III [37]). Therefore, in what follows we consider the ordered structure of $MnBi_2Te_4$.

We start with the magnetic characterization of a single free-standing $MnBi_2Te_4$ SL. The exchange coupling constants J_{0j}, calculated as a function of the Mn-Mn distance $r_{Mn(0)-Mn(j)}$, show the same trend as in bulk $MnBi_2Te_4$ [Fig. 1(b)]. Namely, that the FM interaction between first nearest neighbors, $J_{01} \simeq 0.08$ meV/μ_B^2, strongly dominates over all others. Thus, there is a stable tendency towards the FM ground state in $MnBi_2Te_4$ SL, as confirmed by the total-energy calculations, which show a preference of the FM state over the 120° AFM state by 14.77 meV per Mn pair (Table I). This result is consistent with those of Refs. [14,50], where it has been experimentally shown that each $MnBi_2Te_4$ SL orders ferromagnetically both in bulk and thin films. An FM ground state has also been predicted for a single $MnBi_2Te_4$ SL placed on different tetradymite-like TI substrates [10,11]. Therefore, we conclude that the intralayer FM order is not sensitive to the thickness of the $MnBi_2Te_4$ film, as well as to the formation of the vdW interface with other block-layered compounds.

For the 2-SL-thick film, the total-energy calculations show that the *interlayer* coupling is AFM, leading to the compensated AFM [cAFM; Fig. 1(c)] ordering as in the bulk material [14,18]. Increasing the thickness up to 3 SLs keeps the interlayer exchange coupling antiferromagnetic, but, since the number of blocks is odd, an uncompensated AFM (uAFM; Fig. 1(c)) state arises. Similarly to the 2-SL- and 3-SL-thick films cases, we also predict cAFM and uAFM states for the thicker films composed of even and odd number of SLs, respectively (Table I).

It is well known that the magnetic anisotropy and the interlayer exchange coupling play a crucial role in (quasi-)

TABLE I. Thickness dependence of the $MnBi_2Te_4$ films magnetism. $\Delta E_{A/F} = E_{AFM} - E_{FM}$ is the total energy difference of the AFM and FM states, where AFM refers to the intralayer 120° state [18] in the case of the single SL, while for the thicker films and bulk it means the interlayer AFM state (Fig. 1(c)). cAFM (uAFM) stands for the compensated (uncompensated) AFM state. T_c denotes the Curie or Néel temperature in the FM or AFM cases, respectively. The numbers in brackets indicate the error bar. Details of the Monte Carlo simulations can be found in Supplementary Note I [37].

Thickness (SL)	$\Delta E_{A/F}$ [meV/(Mn pair)]	Order	MAE (meV/Mn)	T_c (K)
1	14.77	FM	0.125	12(1)
2	−1.22	cAFM	0.236	24.4(1)
3	−1.63	uAFM	0.215	
4	−1.92	cAFM	0.210	
5	−2.00	uAFM	0.205	
6	−2.05	cAFM		
7	−2.09	uAFM		
∝ (bulk)	−2.80	cAFM	0.225	25.42(1)

2D magnets. Indeed, if a purely 2D magnet has an easy-plane magnetic anisotropy, it features no magnetic order at any temperature except zero Kelvin according to the Mermin-Wagner theorem [51,52]. The reason for this is the Goldstone mode of the gapless long-wavelength magnetic excitations, whose destructive role increases with decreasing dimensionality of the system. In the limit of strong easy-plane anisotropy, such systems undergo, instead of a second order phase transition, a so-called Berezinskii-Kosterlitz-Thouless transition [53,54], which is manifested in a change of the spin-spin correlation function behavior from a power law below the crossover temperature T_{BKT} to an exponential law above it. It is precisely the interlayer exchange coupling that stabilizes the long-range order at finite temperatures in such cases [55]. Alternatively, even a small gap in the excitation spectrum introduced by the easy-axis magnetic anisotropy can significantly reduce the impact of the low-energy excitations. In this case, the three-dimensional (3D) exchange contribution is expected to further enhance the critical temperature [56].

We then calculate the MAE for the $MnBi_2Te_4$ films from 1 to 5 SLs as well as for bulk (Table I). In all these cases, the MAE is positive, indicating an out-of-plane easy axis in agreement with recent experiments [14,50]. The anisotropy of the SL-thick FM film turns out to be weaker than that of the thicker films with AFM interlayer coupling, for which the MAE was found to be close to the bulk value (see Table I). The magnitudes of the local magnetic moments are practically independent from the film thickness, being roughly equal to 4.6 μ_B in all cases. The Curie temperature of the 1-SL-thick FM film, which represents a purely 2D magnetic system, appears to be approximately equal to 12 K. Because of the appearance of the interlayer exchange

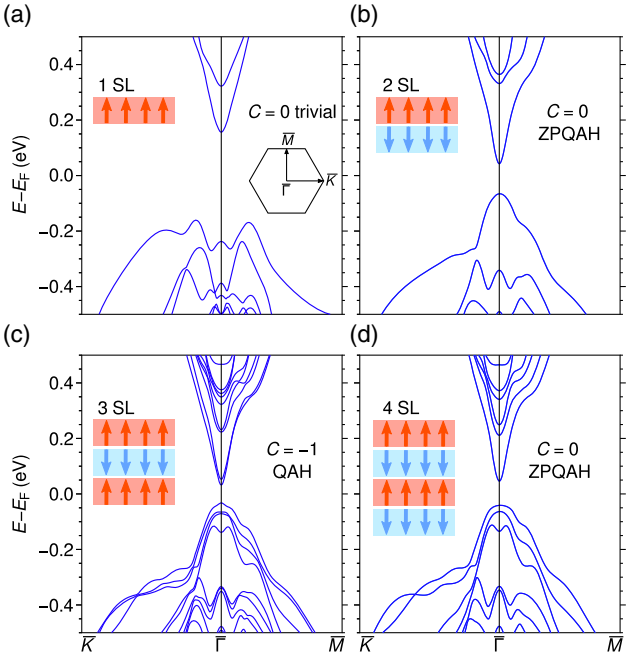

FIG. 2. Electronic band structures of the $MnBi_2Te_4$ films calculated along the $\bar{K}$–$\bar{\Gamma}$–$\bar{M}$ path in the 2D Brillouin zone for different thicknesses: (a) 1 SL, (b) 2 SLs, (c) 3 SLs, and (d) 4 SLs.

coupling and an increase in the MAE, the Néel temperature of a double SL film increases to ≈24.4 K, which is just slightly lower than that of bulk (Table I).

Now we show that in the thin-film limit not only the magnetic, but also the electronic and topological properties of $MnBi_2Te_4$ are strongly thickness dependent. The band structure of the $MnBi_2Te_4$ single SL block is shown in Fig. 2(a). In good agreement with the experimental data [50], it shows an indirect band gap of ∼0.32 eV. Note that a direct gap of 0.73 eV has been calculated in Ref. [57]. The Chern number calculation reveals a $C = 0$ state, the system being a topologically trivial ferromagnet (Table II).

Upon increasing thickness up to 2 SLs the interlayer cAFM order sets in. Because of the inversion symmetry, the bands are doubly degenerate [Fig. 2(b)], which always yields a zero Berry curvature and, therefore, $C = 0$. For this system, we find a band gap of 107 meV. However, if calculated in the artificial FM phase of the 2-SL-thick film, the Chern number appears to be equal to −1, indicating a QAH insulator state. Accordingly, the edge band structure of the system shows a single 1D chiral mode [Fig. 3(a)]. Reversing the magnetization of the FM 2-SL-thick $MnBi_2Te_4$ film yields the $C = +1$ QAH state. These results suggest that the 2-SL-thick cAFM $MnBi_2Te_4$ film is likely to be in a so-called zero plateau QAH (ZPQAH) state. Up to now, the ZPQAH state was an artificial state of a QAH insulator that is realized in the process of the magnetization reversal by an external magnetic field (i.e., during the transition between the two QAH states with Chern numbers of opposite signs). The ZPQAH state manifests itself in the appearance of flat regions in the

TABLE II. Thickness dependence of the $MnBi_2Te_4$ films topology and band gap size. QAH and ZPQAH stand for the quantum anomalous Hall phase and its zero plateau state, respectively.

Thickness (SL)	Topology	Band gap (meV)
1	Trivial	321
2	ZPQAH	107
3	QAH	66
4	ZPQAH	97
5	QAH	77
6	ZPQAH	87
7	QAH	85
$\propto$ (bulk)	3D AFM TI	225

hysteresislike dependence of the Hall conductivity on the external field $\sigma_{xy}(H)$. Namely, within a certain range of H close to the coercivity, the $\sigma_{xy} = 0$ plateau is observed, which corresponds to a fully gapped band structure. Outside this H range, σ_{xy} rapidly reaches a quantized value of either $+e^2/h$ or $-e^2/h$, depending on the magnetization direction. Such a situation can be achieved either in (i) a zero magnetization state of the magnetically doped QAH insulator due to the coexistence of the upwards and downwards magnetized domains [58] or (ii) the antiparallel magnetizations state of an FM1(↑)/TI/FM2(↓) QAH heterostructure, where FM1 and FM2 are two different FM insulators [59]. To check whether the ZPQAH state is realized in the 2-SL-thick $MnBi_2Te_4$ film, we have calculated the edge band structure in the cAFM ground state of the system. We find a fully gapped spectrum [Fig. 3(b)], corresponding to $\sigma_{xy} = 0$. Thus, the 2-SL-thick $MnBi_2Te_4$ film represents the first ever example of an intrinsic ZPQAH phase. Also, these results vividly illustrate the interplay of topology and magnetism: the system could be a $|C| = 1$ QAH insulator, if it was not

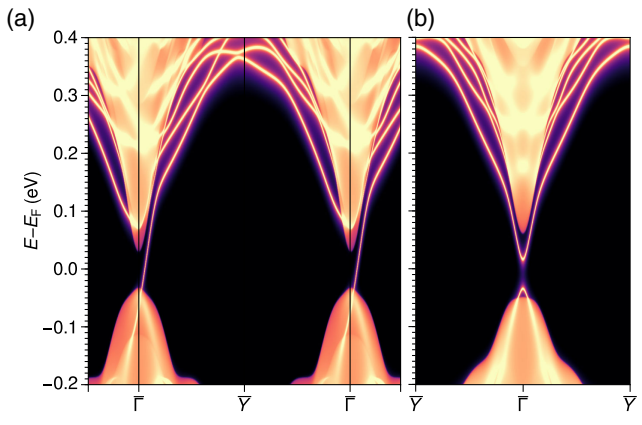

FIG. 3. Edge electronic band structures of the $MnBi_2Te_4$ 2-SL-thick film calculated for the (a) FM and (b) cAFM states. The regions with a continuous spectrum correspond to the 2D bulk states projected onto a 1D Brillouin zone. The edge crystal structure is shown in Supplemental Material I [37].

for the interlayer AFM coupling, which induces a ZPQAH state ($C = 0$).

At a thickness of 3 SLs, the band gap gets inverted due to spin-orbit coupling (Supplemental Material IV [37]), what drives the system in a $C = -1$ QAH insulator state. Similarly to the 2-SL-thick (3-SL-thick) film cases, we also predict the intrinsic ZPQAH (QAH) states for the 4- and 6-SL-thick (5- and 7-SL-thick) films, respectively (Table II).

At this point, having described various phases realized in the $MnBi_2Te_4$ films, it is important to emphasize a crucial advantage of the here proposed (ZP)QAH insulators: they show ordered structures, inherent to the stoichiometric material, which guarantees them against disorder-related drawbacks such as the band gap fluctuation [60] or superparamagnetism [61,62]. This very fact, together with the large band gaps of such systems (Table II), could facilitate the observation of the QAH effect at temperatures notably higher than those achieved so far. This is all the more true since, starting from the 2 SLs thickness, the MAE is already close to that of the bulk. This indicates that the $MnBi_2Te_4$ QAH insulators should have critical temperatures comparable to the bulk Néel temperature of $MnBi_2Te_4$ (Table I). To be mentioned as well is a solid state realization of axion electrodynamics in a ZPQAH state proposed recently [59]. Up to now the axion insulator state was being sought for in the FM1/TI/FM2 QAH heterostructures. In such systems, a relatively thick TI spacer enables magnetization reversal of the individual FM layers that have different coercivities, leading to the overall AFM alignment and, consequently, to a ZPQAH state [63,64]. In contrast to the latter heterostructures, the $MnBi_2Te_4$ thin films made of even number of SLs realize this state intrinsically, i.e., without the need of magnetic field application.

In summary, using *ab initio* and Monte Carlo calculations, we have scrutinized the magnetic, electronic, and topological properties of the $MnBi_2Te_4$ AFM TI thin films. Belonging to the class of layered vdW compounds, in the 2D limit $MnBi_2Te_4$ shows a unique set of thickness-dependent transitions through various phases, being among them wide-band-gap QAH and ZPQAH states. A similar behavior can possibly take place in other compounds of the $MnBi_2Te_4$ family, such as $MnSb_2Te_4$, $MnBi_2Se_4$ [9,13,18], and others. We believe that our findings will stimulate intensive studies of thin films of vdW antiferromagnets as prospective materials for AFM spintronics.

The authors thank J. I. Cerdá, V. N. Men'shov, and V. N. Golovach for stimulating discussions. We acknowledge the support by the Basque Departamento de Educación, UPV/EHU (Grant No. IT-756-13), Spanish Ministerio de Economia y Competitividad (MINECO Grant No. FIS2016-75862-P), Academic D. I. Mendeleev Fund Program of Tomsk State University (Project No. 8.1.01.2018), and Fundamental Research Program of the State Academies of Sciences, line of research III.23. The support by the Saint Petersburg State University for

scientific investigations (Grant No. 15.61.202.2015) and Russian Foundation for Basic Research – RFBR (project 18-52-06009) are also acknowledged. I. P. R. acknowledges support by the Ministry of Education and Science of the Russian Federation within the framework of the governmental program Megagrants (State Task No. 3.8895.2017/P220). This study was supported by Russian Science Foundation No. 18-12-00169 in the part of the calculations within tight-binding method. A. E. acknowledges financial support from DFG through priority program SPP1666 (Topological Insulators) and OeAD Grants No. HR 07/2018 and No. PL 03/2018. The calculations were performed in Donostia International Physics Center, in the Research park of St. Petersburg State University Computing Center [65], and at SKIF Cyberia cluster of Tomsk State University.

*mikhail.otrokov@gmail.com
†evguenivladimirovich.tchoulkov@ehu.eus

[1] M. Z. Hasan and C. L. Kane, Rev. Mod. Phys. **82**, 3045 (2010).
[2] S. V. Eremeev, G. Landolt, T. V. Menshchikova, B. Slomski, Y. M. Koroteev, Z. S. Aliev, M. B. Babanly, J. Henk, A. Ernst, L. Patthey *et al.*, Nat. Commun. **3**, 635 (2012).
[3] X. Xu, W. Yao, D. Xiao, and T. F. Heinz, Nat. Phys. **10**, 343 (2014).
[4] K. Ishizaka, M. Bahramy, H. Murakawa, M. Sakano, T. Shimojima, T. Sonobe, K. Koizumi, S. Shin, H. Miyahara, A. Kimura *et al.*, Nat. Mater. **10**, 521 (2011).
[5] L. Li, Y. Yu, G. J. Ye, Q. Ge, X. Ou, H. Wu, D. Feng, X. H. Chen, and Y. Zhang, Nat. Nanotechnol. **9**, 372 (2014).
[6] A. Banerjee, C. Bridges, J.-Q. Yan, A. Aczel, L. Li, M. Stone, G. Granroth, M. Lumsden, Y. Yiu, J. Knolle *et al.*, Nat. Mater. **15**, 733 (2016).
[7] C. Gong, L. Li, Z. Li, H. Ji, A. Stern, Y. Xia, T. Cao, W. Bao, C. Wang, Y. Wang *et al.*, Nature (London) **546**, 265 (2017).
[8] B. Huang, G. Clark, E. Navarro-Moratalla, D. R. Klein, R. Cheng, K. L. Seyler, D. Zhong, E. Schmidgall, M. A. McGuire, D. H. Cobden *et al.*, Nature (London) **546**, 270 (2017).
[9] T. Hirahara, S. V. Eremeev, T. Shirasawa, Y. Okuyama, T. Kubo, R. Nakanishi, R. Akiyama, A. Takayama, T. Hajiri, S. Ideta *et al.*, Nano Lett. **17**, 3493 (2017).
[10] M. M. Otrokov, T. V. Menshchikova, I. P. Rusinov, M. G. Vergniory, V. M. Kuznetsov, and E. V. Chulkov, JETP Lett. **105**, 297 (2017).
[11] M. M. Otrokov, T. V. Menshchikova, M. G. Vergniory, I. P. Rusinov, A. Yu. Vyazovskaya, Yu. M. Koroteev, G. Bihlmayer, A. Ernst, P. M. Echenique, A. Arnau *et al.*, 2D Mater. **4**, 025082 (2017).
[12] E. K. Petrov, I. V. Silkin, T. V. Menshchikova, and E. V. Chulkov, Pis'ma Zh. Eksp. Teor. Fiz. **109**, 118 (2019).
[13] J. A. Hagmann, X. Li, S. Chowdhury, S.-N. Dong, S. Rouvimov, S. J. Pookpanratana, K. M. Yu, T. A. Orlova, T. B. Bolin, C. U. Segre *et al.*, New J. Phys. **19**, 085002 (2017).
[14] M. M. Otrokov, I. I. Klimovskikh, H. Bentmann, A. Zeugner, Z. S. Aliev, S. Gass, A. U. B. Wolter, A. V. Koroleva, D. Estyunin, A. M. Shikin *et al.*, arXiv:1809.07389.
[15] R. S. K. Mong, A. M. Essin, and J. E. Moore, Phys. Rev. B **81**, 245209 (2010).
[16] R. Li, J. Wang, X.-L. Qi, and S.-C. Zhang, Nat. Phys. **6**, 284 (2010).
[17] Y. Peng and Y. Xu, arXiv:1809.09112.
[18] S. V. Eremeev, M. M. Otrokov, and E. V. Chulkov, J. Alloys Compd. **709**, 172 (2017).
[19] S. V. Eremeev, M. M. Otrokov, and E. V. Chulkov, Nano Lett. **18**, 6521 (2018).
[20] Y. S. Hou and R. Q. Wu, arXiv:1809.09265.
[21] V. Baltz, A. Manchon, M. Tsoi, T. Moriyama, T. Ono, and Y. Tserkovnyak, Rev. Mod. Phys. **90**, 015005 (2018).
[22] P. E. Blöchl, Phys. Rev. B **50**, 17953 (1994).
[23] G. Kresse and J. Furthmüller, Phys. Rev. B **54**, 11169 (1996).
[24] G. Kresse and D. Joubert, Phys. Rev. B **59**, 1758 (1999).
[25] J. P. Perdew, K. Burke, and M. Ernzerhof, Phys. Rev. Lett. **77**, 3865 (1996).
[26] D. D. Koelling and B. N. Harmon, J. Phys. C **10**, 3107 (1977).
[27] S. Grimme, J. Antony, S. Ehrlich, and H. Krieg, J. Chem. Phys. **132**, 154104 (2010).
[28] S. Grimme, S. Ehrlich, and L. Goerigk, J. Comput. Chem. **32**, 1456 (2011).
[29] V. I. Anisimov, J. Zaanen, and O. K. Andersen, Phys. Rev. B **44**, 943 (1991).
[30] S. L. Dudarev, G. A. Botton, S. Y. Savrasov, C. J. Humphreys, and A. P. Sutton, Phys. Rev. B **57**, 1505 (1998).
[31] E. Wimmer, H. Krakauer, M. Weinert, and A. J. Freeman, Phys. Rev. B **24**, 864 (1981).
[32] FLEUR site, http://www.flapw.de.
[33] A. A. Soluyanov and D. Vanderbilt, Phys. Rev. B **83**, 235401 (2011).
[34] D. Gresch, G. Autès, O. V. Yazyev, M. Troyer, D. Vanderbilt, B. A. Bernevig, and A. A. Soluyanov, Phys. Rev. B **95**, 075146 (2017).
[35] N. Marzari and D. Vanderbilt, Phys. Rev. B **56**, 12847 (1997).
[36] A. A. Mostofi, J. R. Yates, Y.-S. Lee, I. Souza, D. Vanderbilt, and N. Marzari, Comput. Phys. Commun. **178**, 685 (2008).
[37] See Supplemental Material at http://link.aps.org/supplemental/10.1103/PhysRevLett.122.107202 for a detailed description of methods, interlayer AFM coupling mechanism, total-energy calculations for the structures with Mn/Bi intermixing, and band gap inversion in $MnBi_2Te_4$ thin films, which includes Refs. [38–47].
[38] M. P. Lopez Sancho, J. M. Lopez Sancho, J. M. L. Sancho, and J. Rubio, J. Phys. F **15**, 851 (1985).
[39] J. Henk and W. Schattke, Comput. Phys. Commun. **77**, 69 (1993).
[40] D. J. Thouless, M. Kohmoto, M. P. Nightingale, and M. den Nijs, Phys. Rev. Lett. **49**, 405 (1982).
[41] Y. Yao, L. Kleinman, A. H. MacDonald, J. Sinova, T. Jungwirth, D.-S. Wang, E. Wang, and Q. Niu, Phys. Rev. Lett. **92**, 037204 (2004).
[42] L. M. Sandratskii and P. Bruno, Phys. Rev. B **66**, 134435 (2002).
[43] M. Lezaic, Ph. Mavropoulos, J. Enkovaara, G. Bihlmayer, and S. Blügel, Phys. Rev. Lett. **97**, 026404 (2006).

[44] V. I. Anisimov, F. Aryasetiawan, and A. I. Lichtenstein, J. Phys. Condens. Matter **9**, 767 (1997).
[45] A. B. Shick, A. I. Liechtenstein, and W. E. Pickett, Phys. Rev. B **60**, 10763 (1999).
[46] V. I. Anisimov, I. V. Solovyev, M. A. Korotin, M. T. Czyżyk, and G. A. Sawatzky, Phys. Rev. B **48**, 16929 (1993).
[47] H. J. Monkhorst and J. D. Pack, Phys. Rev. B **13**, 5188 (1976).
[48] D. S. Lee, T.-H. Kim, C.-H. Park, C.-Y. Chung, Y. S. Lim, W.-S. Seo, and H.-H. Park, CrystEngComm **15**, 5532 (2013).
[49] P. W. Anderson, Phys. Rev. **115**, 2 (1959).
[50] Y. Gong *et al.*, arXiv:1809.07926.
[51] N. D. Mermin and H. Wagner, Phys. Rev. Lett. **17**, 1133 (1966).
[52] M. Bander and D. L. Mills, Phys. Rev. B **38**, 12015 (1988).
[53] V. Berezinskii, Sov. Phys. JETP **32**, 493 (1971).
[54] J. M. Kosterlitz and D. J. Thouless, J. Phys. C **6**, 1181 (1973).
[55] A. A. Katanin and V. Y. Irkhin, Phys. Usp. **50**, 613 (2007).
[56] M. M. Otrokov, G. Fischer, P. Buczek, A. Ernst, and E. V. Chulkov, Phys. Rev. B **86**, 184418 (2012).
[57] J. Li *et al.*, arXiv:1808.08608.
[58] J. Wang, B. Lian, and S.-C. Zhang, Phys. Rev. B **89**, 085106 (2014).
[59] J. Wang, B. Lian, X.-L. Qi, and S.-C. Zhang, Phys. Rev. B **92**, 081107 (2015).
[60] I. Lee, C. K. Kim, J. Lee, S. J. L. Billinge, R. Zhong, J. A. Schneeloch, T. Liu, T. Valla, J. M. Tranquada, G. Gu *et al.*, Proc. Natl. Acad. Sci. U.S.A. **112**, 1316 (2015).
[61] E. O. Lachman, A. F. Young, A. Richardella, J. Cuppens, H. Naren, Y. Anahory, A. Y. Meltzer, A. Kandala, S. Kempinger, Y. Myasoedov *et al.*, Sci. Adv. **1**, e1500740 (2015).
[62] J. A. Krieger, C.-Z. Chang, M.-A. Husanu, D. Sostina, A. Ernst, M. M. Otrokov, T. Prokscha, T. Schmitt, A. Suter, M. G. Vergniory *et al.*, Phys. Rev. B **96**, 184402 (2017).
[63] M. Mogi, M. Kawamura, A. Tsukazaki, R. Yoshimi, K. S. Takahashi, M. Kawasaki, and Y. Tokura, Sci. Adv. **3**, eaao1669 (2017).
[64] D. Xiao, J. Jiang, J.-H. Shin, W. Wang, F. Wang, Y.-F. Zhao, C. Liu, W. Wu, M. H. W. Chan, N. Samarth *et al.*, Phys. Rev. Lett. **120**, 056801 (2018).
[65] http://cc.spbu.ru.